Active Generation Network of Human Skeleton for Action Recognition

Long Liu *

liulong@xaut.edu.cn

Xin Wang

wangxin2168@163.com

Fangming Li

2220321220@stu.xaut.edu.cn

Jiayu Chen

cjy21123@163.com

Abstract

Data generation is a data augmentation technique for enhancing the generalization ability for skeleton-based human action recognition. Most existing data generation methods face challenges to ensure the temporal consistency of the dynamic information for action. In addition, the data generated by these methods lack diversity when only a few training samples are available. To solve those problems, We propose a novel active generative network (AGN), which can adaptively learn various action categories by motion style transfer to generate new actions when the data for a particular action is only a single sample or few samples. The AGN consists of an action generation network and an uncertainty metric network. The former, with ST-GCN as the Backbone, can implicitly learn the morphological features of the target action while preserving the category features of the source action. The latter guides generating actions. Specifically, an action recognition model generates prediction vectors for each action, which is then scored using an uncertainty metric. Finally, UMN provides the uncertainty sampling basis for the generated actions.

1. Introduction

Human action recognition (HAR) is one of the hotspots in computer vision, widely applied to intelligent surveillance, human-computer interaction, and virtual reality [2, 14, 22, 63]. The main methods are RGB-based, RGBD-based, and Skeleton-based [7, 15, 16, 31, 36, 67]. In contrast, the Skeleton is a simple structure that is robust to changes in appearance features, complex backgrounds, and occlusion interference in RGB data. Therefore, Skeleton-based HAR is gradually becoming a mainstream method.

In recent years, graph convolutional networks (GCN) [4, 6, 56, 65] have rapidly developed to extract spatio-temporal relationships among joints. Applications of GCNs have achieved outstanding performance in skeleton-based HAR. These results are largely dependent on the availability of large amounts of data. However, human action data can only be obtained for a few or even one sample because of privacy, low probability of occurrence, and high cost, e.g., cheating on exams, robbery, and homicide. These issues limit the quantity of human action data, thereby limiting the generalization ability of HAR. With the continuous development of data generation techniques, the possibility of generating large datasets has emerged.

The traditional data generation methods include geometric transformations, noise injection, and data interpolation [23, 57]. The original data limits this method, cannot generate new data, and is easily distorted. Subsequently, many deep learning-based data generation methods have been proposed, such as generative adversarial networks (GAN) [8, 9, 32, 33, 62], variational autoencoders (VAE) [35, 39, 40], flow models [34, 51], and diffusion models [24, 38, 71]. These methods are effective only for generating static data such as images and text [37, 42, 50]. However, for dynamic data such as human actions, the generated actions may be unnatural and discontinuous between frames and lack temporal consistency. In addition, when only a few training samples are available, it leads to a poor generalization of the generated model, and the generated data lacks diversity. Few-shot generation approaches [3, 10, 17, 26–28, 46] aim to generate a large amount of natural and diverse data for a few new categories, partly solving this problem. However, the method mainly uses a small number of samples for data generation and does not utilize the rich information of many base categories. Many base category action for human actions have more complete data distribution information. Incorporating this feature information into the generation process can provide richer features for new actions.

To address the above, motion style transfer provides an excellent solution. Motion style transfer [1, 25, 30, 48] aims to extract the target style from a action example and transfer it to another action with the desired content. The problem of temporal consistency is improved by the adaptive instance normalization (AdaIN) [29, 52] aligning the two action features rather than simply fusing them. The recent work by

JANG et al. [30] proposes a novel motion style transfer network. The network consists of multi-layer ST-GCNs that can achieve arbitrary motion transfer without style labeling. Our work follows the same approach. Motion Puzzle divides the human skeleton into five parts, allowing flexible control over the migration of specified parts during generation. This approach is effective for single-action generation tasks. However, it is usually time-consuming to control parts for generation when generating many actions. In addition, Motion Puzzle's target motion encoder is connected to the decoder at multiple scales, which may constrain the diversity of action. Although motion style transfer is a generative network, it is not designed to solve the problem of data sparsity but is purely a one-to-one feature transfer. The quality of generation is only partially guaranteed when generating lots of data. To this end, we select and utilize the most informative samples by incorporating active learning [12, 59, 70] to guide human action generation.

In this paper, a novel action generation network called Active Generation Network (AGN) is proposed for skeleton data generation. Our method adaptively learns various action categories by motion style transfer. With only a few or even a single sample, AGN can generate many new actions without assigning body parts. A unique advantage is incorporating active learning into the generation process. For a large number of action samples generated, the most valuable samples are implicitly selected using an uncertainty metric in active learning to ensure the quality of the generation. To the best of our knowledge, our work is the first that guides the generation of human actions using active learning.

The AGN consists of a action generation network (AcGN) and an uncertainty metric network (UMN). The MGN consists of two encoders and a decoder. The encoders extract action features by the graph convolution layer and instance normalization layer, and then the decoder synthesizes new actions. The MGN can implicitly learn the skeletal morphology of the target actions without stylizing any actions while preserving the categories of the original actions. Inspired by active learning, we developed UMN to guide the MGN. Firstly, we train ST-GCN using a few or a single sample to generate prediction vectors for new actions. Then, a score is obtained from the uncertainty metric, based on which samples are selected and added to the train set to train the ST-GCN again. This process is repeated until the data meets the requirements.

The contributions of our work can be summarized as follows:

- We propose a generative network called MGN for skeletal data to generate high-quality human action data with only a few or a single sample.
- We propose AGN for Human Skeletons for HAR. Introducing active learning into the generation process implic-

itly selects the most valuable samples using an uncertainty metric to ensure the generation quality.
- FMD and Accuracy are used to evaluate the results on the NTU-RGB+D dataset. The results show that our method is competitive with other methods. The method requires only 10% of the original data for the same accuracy.

2. Related work

Generative Adversarial Networks. Generative Adversarial Networks (GAN) is a generative models which is trained by adversarial learning. In the early days, unconditional GAN [32, 33] recovered images from random noise. Developed to the present, conditional GAN [47] utilizes text and images for guidance to generate images. GAN has performed strongly on tasks of generating static data such as image generation [32, 33], image editing [49, 60], and image translation [55]. The generation of dynamic data, such as videos and action sequences, has also been studied. Carl et al. [61] proposed a video generation network with a spatial-temporal two-stream convolutional architecture based on DCGAN [50]. This work is the first application of GAN to video generation. TGAN [53] followed, which first generates a set of latent vectors from noise vectors, then generates pictures and synthesizes videos separately. RNN-GAN [44] is based on the temporal modeling capability of RNNs to predict video from a single frame. It has a more robust motion prediction capability compared to the work of Carl et al. However, these impressive results are mainly attributed to the support of many training samples. With limited data, GANs are prone to overfitting, leading to a lack of diversity in the generated data.

Motion Style Transfer. Image Style Transfer [20, 52] combines style and content features from two images to form a new image. Motion Style Transfer refers to Image Style Transfer to form a new action by transferring one action's style features to another that contains only content features. Early motion style transfer was done by manually defining style features and inferring them through machine learning [64, 69]. This method is effective only for the actions in the training data with limited scope of usefulness. Deep learning-based methods have greatly improved the quality and application of motion style transfer. Both Holden et al. [25] and Du et al. [11] applied the Gram matrix method to convey motion styles through the distribution of actions in the hidden space. These methods are time-consuming and have limited the quality of action generation for relatively significant motion differences. Recently, Aberman et al. [1] proposed a motion transfer network that combines GAN and AdaIN. The method can learn from unpaired data with different styles to migrate model unseen actions. Park et al. [48] used a spatio-temporal graph convolutional network to model actions. The method adds random noise in the decoder to enhance action diversity. Jang et al.

[30] proposed a novel motion style transfer network called Motion Puzzle. Motion Puzzle divides the human skeleton into five parts, allowing flexible control over the migration of specified parts during generation. This approach is effective for single-action generation tasks. However, it is usually time-consuming to control parts for generation when generating many actions. In addition, Motion Puzzle's target motion encoder is connected to the decoder at multiple scales, which may constrain the diversity of action.

Active Learning. Existing active learning methods are categorized into pool-based and synthetic methods [5, 18, 21, 45, 68]. Pool-based methods use different sampling strategies to determine how to select the most informative samples, with uncertainty sampling methods being the most common. Ebrahimi et al. [13] used a Bayesian neural network for uncertainty evaluation. Gal [18] and Gharamani [19] also showed the relationship between uncertainty and dropout to estimate uncertainty in neural network prediction. Pool-based methods select samples conditional on a large amount of unlabeled data. In the case of scarcity of data, synthetic methods are more suitable than pool-based methods. Synthetic methods use a generative model to generate samples, then sample based on the uncertainty of the model. The work of Zhu et al. [72], Mahapatra et al. [41], and Mayer et al. [43] uses GAN to generate a sample and then query using the uncertainty principle. Our work uses this same strategy to guide human action generation using the amount of sample information.

3. Method

3.1. Overview

Figure 1 shows the overall architecture of the AGN framework, consisting of MGN and UMN. The MGN generates new actions, and the UMN evaluates the generated actions and inversely guides the generation of MGN. We construct a human action set $\mathcal{M} = \mathcal{M}_{train} \cup \mathcal{M}_{unseen}$ using 3D skeletal data from NTU-RGB+D 60 [54], where $\mathcal{M}_{train} \cap \mathcal{M}_{unseen} = \varnothing$. In addition, we define different action subsets. The AGN's input is a complete target action set $\mathcal{M}_{full}$ and a one-shot or few-shot source action set $\mathcal{M}_{few}$. The final output is a complete action set $\mathcal{M}_{gen}$ of equal size $\mathcal{M}_{full}$. The action is denoted as $\mathbf{M}_{src} \in \mathcal{M}_{few}, \mathbf{M}_{tgt} \in \mathcal{M}_{full}$, and $\mathbf{M}_{gen} \in \mathcal{M}_{gen}$.

The MGN uses spatio-temporal graph convolutional layers as the basis to construct the encoder and decoder, connecting the high and low dimensional feature layers of the human skeletal graph structure by graph upsampling and downsampling [30, 66]. The encoder extracts features for the skeletal morphology and the category information of the action, respectively. The decoder outputs the new action by fusing the multi-scale spatio-temporal features of the source and target actions via the BP-StyleNet Layer [30].

The UMN guides the MGN to generate high-quality action. Specifically, the UMN obtains the a posteriori probability of each action via a recognition network. Then, the uncertainty score is obtained via an uncertainty metrics layer to provide a basis for sample selection.

3.2. Action Generation Network

Graph Upsampling and Downsampling. A practical method for extracting features in image generation is progressive upsampling and downsampling. The upsampling gradually improves the image resolution and increases the local details, and the downsampling can aggregate the image features and reduce the noise. The upsampling and downsampling are generally implemented through Unpooling and Pooling. It proved effective in graph convolutional neural networks for skeletal data[30, 48, 66]. Following this idea, we incorporate the upsampling and downsampling methods combined with information entropy into the spatial-temporal graph to extract local and global features.

Action Encoder. We developed the action encoder similar to VGG16 [58] to map human actions to latent space using graph upsampling and spatio-temporal graph convolutional layers. Given an action $\mathbf{M}_s$, the encoding process is written as:

$$z_s = E_s(\mathbf{M}_s), \tag{1}$$

where $s \in \{src, tgt\}$. The action encoder consists of a source encoder and a target encoder. Each encoder E_s is a concatenation of multi-level encoding blocks E_s^i to gradually extract the latent feature $z_s^i = E_s^i(z_s^{i-1})$, where $i \in \{1, 2, 3\}$, and z_s^i is the action feature obtained after each encoding block.

The source encoding block E_{src}^i consists of instance normalization layer (IN), ST-GCN, and graph downsampling (GD) to extract source action features gradually. In the target encoder, we wish to preserve the morphological features of the action to combine with the category features of the source action to form a unique new action. Therefore, it consists only of ST-GCN and GD.

Feature Decoder. The feature decoder fuses the category features z_{src} of the source action with the morphological features z_{tgt} of the target action to synthesise a new action $\mathbf{M}_{gen}$. The dncoding process is written as:

$$\mathbf{M}_{gen} = D(z_{src}, z_{tgt}). \tag{2}$$

The decoder is similar in structure to the encoder and consists of three decoding blocks and three linear layers. The three decoding blocks recover the action sequences step-by-step by fusing z_{tgt} and $\hat{z}_{dec}^0(= z_{src})$, defined as:

$$\hat{z}_{dec}^i = D^i(\hat{z}_{dec}^{i-1}, L^i(z_{tgt})), \tag{3}$$
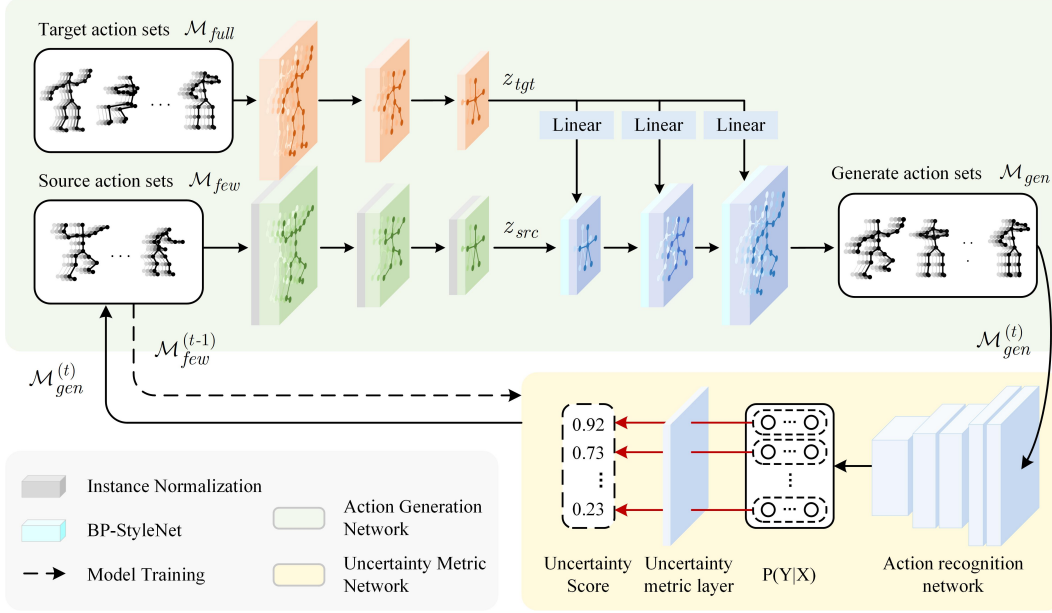
3

Figure 1. The overall network architecture of our AGN framework.

where $i \in \{1, 2, 3\}$, $\hat{z}_{dec}^i$ is the action feature output from each decoding block, and L^i is the linear layer mapping the deep feature z_{tgt} to the same feature map size as the output of each decoding blocks.

We use Body Part Adaptive Instance Normalisation (BP-AdaIN) and Body Part Attention Network (BP-ATN) in the decoding block from Motion Puzzle [30], where BP-AdaIN applies AdaIN [20, 52] according to the body parts, extending the network's degree of freedom, and more flexible fusion of the features of each part of the target and the source action. The BP-ATN constructs the feature attention mapping of the target and source actions. BP-AdaIN and BP work together to extract local and global features of the target action.

3.3. Uncertainty Metric Network

Action Recognition Network. The prediction vectors are obtained from the action recognition model, thereby calculating the uncertainty score. Our task is oriented towards data generation for action recognition, and thus, ST-GCN is adopted as the task model. At the first iteration, $\mathcal{M}_{gen}^{(1)} = MGN(\mathcal{M}_{few}^{(0)}, \mathcal{M}_{full})$ is obtained by inputting $\mathcal{M}_{few}^{(0)}$ into the MGN. Meanwhile, the task model is trained using $\mathcal{M}_{few}^{(0)}$. Finally, prediction vectors are generated for each action. Starting from the second iteration, $\mathcal{M}_{few}^{(t)} = \mathcal{M}_{few}^{(t-1)} \cup \mathcal{M}_{gen}^{(t)}, t \in [1, iter]$. Given that the number of categories is L, then $Y = p(\mathcal{M}_{gen}^{(t)} | \mathcal{M}_{few}^{(t-1)}) \in \mathbb{R}^{K \times L}$, where K is the number of generating samples, and $p(A|B)$ denotes the prediction vectors produced by the action recog-

nition model trained under dataset B for dataset A.

Uncertainty Metrics. The uncertainty score of the prediction vector is calculated by the uncertainty metric. The uncertainty score is calculated as follows:

$$S(Y) = I - \frac{Var(Y'[k])}{Var(Y[k])} \times max(Y[k]), \quad (4)$$

where I is a full one-vector of length K, then $S(Y) \in \mathbb{R}^K, k \in [1, K]$. The $Var(Y[k])$ can be formulated as:

$$Var(Y[k]) = \frac{1}{L} \sum_l (Y[l, k] - \frac{1}{L})^2. \quad (5)$$

The $Var(Y'[k])$ is the minimum variance of the same vector as the maximum value of $Y[k]$, denoted as:

$$Var(Y'[k]) =$$
$$\frac{1}{L}((max(Y[k]) - \frac{1}{L})^2 + (L-1)(\frac{1 - max(Y[k])}{L - 1} - \frac{1}{L})^2). \quad (6)$$

The maximum value in $Y'[k]$ is the same as the maximum value of $Y[k]$, and the other elements are $\frac{1 - max(Y[k])}{L - 1}$. Therefore, $\frac{Var(Y'[k])}{Var(Y[k])}$ represents the degree of concentration of the probability distribution of the predicted vectors. It ensures that each score ranges from 0 to 1 and is negatively correlated with the maximum vector, i.e., a smaller $max(Y[k])$ indicates greater uncertainty. Finally, the action data is selected based on this score to form the action set $\mathcal{M}_{gen}$.

4

3.4. Training

We train the action generation network end-to-end, given the source action $\mathbf{M}_{src} \in \mathcal{M}_{src}$ and the target action set $\mathbf{M}_{tgt} \in \mathcal{M}_{tgt}$, and optimize the network with the following loss function.

Reconstruction loss and **Cycle consistency loss** are outstanding in motion style transfer [1, 25, 30, 48]. Reconstruction loss gives the network the ability to reconstruct a movement. For each action in the action set, the network can reconstruct the action after feature disentanglement and feature fusion. The new action should have both source action category features and target action morphological features. Therefore, the encoders E_{src} and E_{tgt} are used to disentangle the features of $\mathbf{M}_{gen}$ and the acquired features are used to compute the cycle consistency loss with the features of the source and target actions, respectively.

Feature triplet loss. In order to make the category features of the action more apparent in the latent space, a triplet loss is used during training to make the same category of actions clustered with each other and different categories of actions far away from each other so that the network captures the similarities and differences between action features.

$$
\begin{aligned}
\mathcal{L}_{trip} = \\
\mathbb{E}_{\mathbf{M}_i^t, \mathbf{M}_j^t, \mathbf{M}_k^s \sim \mathcal{M}}(||E_{src}(\mathbf{M}_i^t) - E_{src}(\mathbf{M}_j^t)|| - \\
||E_{src}(\mathbf{M}_i^t) - E_{src}(\mathbf{M}_k^s)|| + \delta),
\end{aligned}
\tag{7}
$$

where $\mathbf{M}_i^t$ and $\mathbf{M}_j^t$ represent two motions of the same category, $\mathbf{M}_{i,j}^t$ and $\mathbf{M}_k^s$ denote two motions of the different category, so $t \neq s, i \neq j \neq k$. The boundary value $\delta = 5$.

The total objective function of the MGN is thus:

$$
\mathcal{L}_{total} = \lambda_{rec}\mathcal{L}_{rec} + \lambda_{cyc}\mathcal{L}_{cyc} + \lambda_{trip}\mathcal{L}_{trip},
\tag{8}
$$

where λ_{rec}, λ_{cyc}, and λ_{trip} are the hyperparameters of each loss term. 1, 0.5, and 0.5, respectively, in our experiments.

4. Experiments

We conducted various experiments to prove the effectiveness of the present method. Firstly, we qualitatively measure the results of our method on seen and unseen data, including action visualization and data downscaling visualization. Secondly, the generation quality and accuracy of action recognition were quantitatively measured for the six categories of target actions. Finally, we performed comparison experiments with previous methods and ablation experiments with a special training loss term. In addition, we train the ST-GCN using generated and real data, respectively, and test the accuracy of the same real data, thus evaluating the degree of approximation between the generated and real data.

4.1. Action Generation

Qualitative evaluation. Figure. 2 shows the generated seen actions. (a) and (b) are the "Reach into Pocket" and "Hopping" actions generated with reference to "Brush Hair", respectively, the former being a hand motion and the latter a whole-body motion. (c) and (d) are the "Put Palms Together" and "Bow" actions generated with reference to "Hopping", respectively. All the above actions preserve the source action $\mathbf{M}_{src}$ category features and target action $\mathbf{M}_{tgt}$ morphological features. Compared with Motion Puzzle, this method can generate hand, upper limb, and whole body actions without specifying body parts. Meanwhile, the temporal consistency of the actions is guaranteed, e.g., the real and generated "Hopping" are jumping at the same time in (b), and the bending tendency of the generated and real actions are consistent in (d).

Figure. 3 shows the generated unseen motions. It contains three cases: only the source action is unseen, only the target action is unseen, and both are unseen to thoroughly verify the transfer effect of unseen actions. In (a) and (f), the source action $\mathbf{M}_{src}$ ("Drink Water" and "Jump Up") is unseen, while the target action $\mathbf{M}_{tgt}$ ("Kicking Something") is seen. The generated action $\mathbf{M}_{gen}$ can keep the category information of the source action. In (c) and (d), $\mathbf{M}_{src}$ is seen, and $\mathbf{M}_{tgt}$ is unseen. In $\mathbf{M}_{gen}$, the morphological features of $\mathbf{M}_{tgt}$ are transferred, and the "Kicking Something" action of $\mathbf{M}_{src}$ is retained. Both source and target actions are unseen in (b) and (e). $\mathbf{M}_{gen}$ shows that the model is still able to extract the category information of $\mathbf{M}_{src}$ and the morphology information of $\mathbf{M}_{tgt}$ to form a new action. From the generated actions in Figure. 3, our model can still generate high-quality actions that are unseen for the model.

In order to verify the approximation between the generated data and the real data, t-SNE was used to visualize the action data. Figure. 4 shows the data distribution after dimensionality reduction using t-SNE. The black and red samples in the figure are the source actions, where red is a random sample in black. Cyan samples are the target actions, while green are the generated samples. The six figures show that the distribution of new actions generated using only one source action is similar to the distribution of source actions. The results show that our generated data can replace the original data.

Quantitative evaluation. We quantitatively measured the quality of generation and accuracy of action recognition on seen and unseen data. Specifically, we use two metrics: Fréchet Motion Distance (FMD) and Accuracy (Acc). We compute FMD and Acc on the action set based on all possible combinations of source and target actions generated by the MGN.

The FMD measures the similarity between the feature vectors of real and generated actions, similar to the Fréchet Inception Distance (FID). The action classifier is trained by
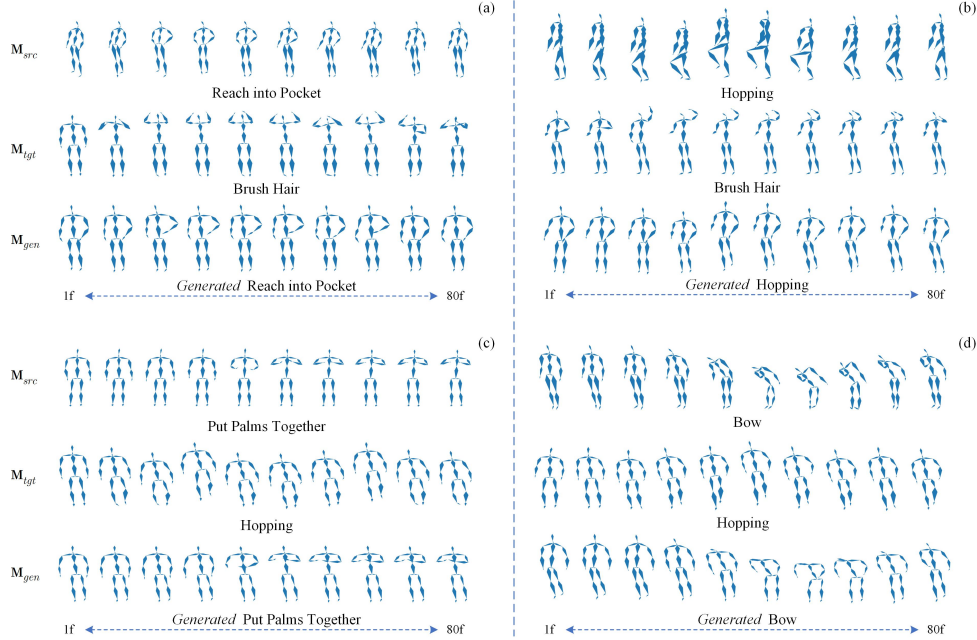
Figure 2. Results generated by MGN on seen actions. (a) "Reach into Pocket". (b) "Hopping". (c) "Put Palms Together". (d) "Bow".

Figure 3. Results generated by MGN on unseen actions. (a) and (b) are "Drink water" (Unseen). (c) and (d) are "Kicking Something" (Seen). (e) and (f) are "Jump Up" (Unseen).

the ST-GCN method, and feature vectors are obtained after the maximum pooling layer to compute the FMD of generated and real actions. A lower FMD means a higher quality of action.

We complete the experimental evaluation using the action sets $\mathcal{M}_{full}$, $\mathcal{M}_{seen}$, and $\mathcal{M}_{unseen}$. The $\mathcal{M}_{seen}$ contains six categories of seen actions data: "Brush Teeth",

"Pick up", "Reading", "Take off a Hat", "Kicking Something", and "Sneeze", for 3996 samples. The $\mathcal{M}_{unseen}$ contains six categories of unseen actions data: "Drink Water", "Throw", "Sit Down", "Clapping", "Jump up", and "Bow", for 3992 samples. Table 1 shows that the Acc of the generated actions all exceeded 90%. The highest of these is 95.39%, with an average of 92.18% under the seen actions
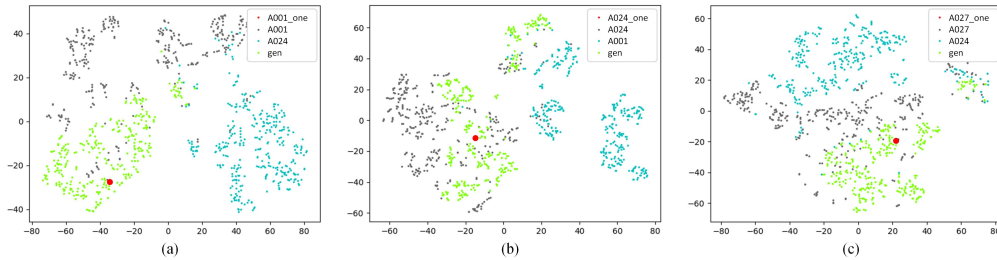
Figure 4. Action data is projected into 2D space using t-SNE, where black is the source action, red is a sample of black, cyan is the target action, and green is some new action generated using a sample of red and some cyan. The green sample and the black sample are very close to each other in space, which indicates that the generated actions conform to some extent to the distribution of the source actions.

	Metric	Target motion					
		A0	A1	A2	A3	A4	A5
Seen	Acc(%)	91.10	90.12	94.63	92.29	95.39	89.54
	FMD	2.19	2.00	1.95	2.02	2.18	2.31
Unseen	Acc(%)	97.20	96.45	89.62	90.78	96.77	95.72
	FMD	3.21	2.49	2.53	3.11	2.30	2.35

Table 1. Quantitative evaluation. We calculated FMD and Acc using $\mathcal{M}_{full}$, $\mathcal{M}_{seen}$, and $\mathcal{M}_{unseen}$. $\mathcal{M}_{full}$ contains six categories of action: "Brush Hair", "Writing", "Put on a Shoe", "Take off Glasses", "Hopping", and "Shake Head". For representation simplicity, we numbered the six categories of target action as A0, A1, A2, A3, A4, and A5.

Target motion	OneShot(%)	FewShot(%)			$\mathcal{M}_{tr\hat{a}in}$(%)
		1%	5%	10%	
A0	62.84	84.09	88.34	91.62	
A1	53.31	79.54	89.74	90.04	
A2	57.62	78.14	89.01	91.32	91.80
A3	57.07	81.30	89.25	91.44	
A4	45.96	82.33	88.16	91.14	
A5	61.57	83.49	88.46	91.01	

Table 2. Top-1 accuracy comparison. Sampling one-shot and few-shot (1%, 5%, and 10%) from $\mathcal{M}_{tr\hat{a}in}$ for action generation. The generated and sampled actions are concatenated into a new train set to train and test the ST-GCN.

data. The highest of these is 97.20%, with an average of 94.42% under the unseen actions data. The mean values of FMD in both cases are 2.11 and 2.67, respectively. This shows that our generated actions are high-quality and can be well recognized by the action classifier.

4.2. Action Recognition

Generating compelling and high-quality data is significant for action recognition tasks when specific action categories are scarce. In order to measure the degree of similarity between generated and real data fully, an action recognition model is trained using generated and real actions, respectively.

We divided the actions in $\mathcal{M}_{unseen}$ into a training set $\mathcal{M}_{tr\hat{a}in}$ and a test set $\mathcal{M}_{t\hat{e}st}$. An action recognition model (ST-GCN) is trained using $\mathcal{M}_{tr\hat{a}in}$ and tested on $\mathcal{M}_{t\hat{e}st}$. As shown in the Table 2, the top-1 accuracy is 91.80%. We sample one-shot and few-shot (1%, 5%, and 10%) from $\mathcal{M}_{tr\hat{a}in}$ for action generation. Subsequently, the generated and sampled actions are concatenated into a new train set to train and test the ST-GCN. As shown in Table 2, the top-1 accuracy is highest at 91.62% when sampling 10%, which is only 0.18% lower than that of $\mathcal{M}_{tr\hat{a}in}$. When sampling 1% and 5%, the top-1 accuracy is still high, close to 90%. However, the top-1 accuracy is lower when sampling one,

with a maximum of only 62.84%. This result is expected because when sampling a single sample, the generative model is very limited to learning the source data distribution, leading to a large deviation of the generated data distribution from the original complete data distribution.

4.3. Ablation Study and Comparison with Prior Work

We conduct an ablation study of the loss term and a comparison with other methods to verify the validity of the loss term in the model and the state-of-the-art of our method. Specifically, we quantitatively measure the generation quality and Accuracy of the five generative models: [Aberman et al. 2020], [Jang et al. 2022], MGN($\mathcal{L}_{rec} + \mathcal{L}_{cyc}$), MGN($\mathcal{L}_{rec} + \mathcal{L}_{cyc} + \mathcal{L}_{trip}$), and AGN (Table. 3). Where MGN($\mathcal{L}_{rec} + \mathcal{L}_{cyc} + \mathcal{L}_{trip}$) is a part of AGN. Therefore, the FMD is both 2.67. Due to the effect of UMN, the recognition accuracy of AGN is 4.76% higher than the former, which is 87.42% and 92.18%, respectively. The FMD and Accuracy are 2.90 and 83.43% for the MGN without $\mathcal{L}_{trip}$, proving that our design of $\mathcal{L}_{trip}$ is effective in generative networks. The method of Aberman et al. measures the FMD to be 21.36 and the Accuracy to be 51.34%. Motion Puzzle measured an FMD of 9.42 and an Accuracy of 67.63%. In comparison, our method is competitive.

7

Figure 5. Comparison results. We used four methods to generate hand action ("Drinking Water"), leg action ("Kicking Something"), and whole-body action ("Jump up").

Methods	FMD↓	Acc(%)↑
[Aberman et al. 2020]	21.36 ± 2.37	51.34 ± 1.92
[Jang et al. 2022]	9.42 ± 0.72	67.63 ± 3.95
MGN ($\mathcal{L}_{rec} + \mathcal{L}_{cyc}$)	2.90 ± 0.54	83.43 ± 3.21
MGN ($\mathcal{L}_{rec} + \mathcal{L}_{cyc} + \mathcal{L}_{trip}$)	2.67 ± 0.37	87.42 ± 2.24
AGN (Ours)	$\mathbf{2.67 \pm 0.37}$	$\mathbf{92.18 \pm 2.75}$

Table 3. FMD and Acc are measured using five methods: [Aberman et al. 2020], [Jang et al. 2022], MGN($\mathcal{L}_{rec} + \mathcal{L}_{cyc}$), MGN($\mathcal{L}_{rec} + \mathcal{L}_{cyc} + \mathcal{L}_{trip}$), and AGN.

	A0	A1	A2	A3	A4	A5
MGN($\mathcal{L}_{total}$)	58.29	62.72	74.62	57.32	67.88	68.91
MGN($\mathcal{L}_{total}$)+UMN	84.09	79.54	78.14	81.30	82.33	83.49

Table 4. Comparison of Top-1 accuracy of MGN($\mathcal{L}_{total}$) and MGN($\mathcal{L}_{total}$)+UMN. Sampling 1% from $\mathcal{M}_{tr\hat{a}in}$ for action generation.

Figure. 5 shows the actions generated by the four methods: (a) the actions generated by Aberman's method, (b) the actions generated by Motion Puzzle, (c) the actions generated by MGN ($\mathcal{L}_{trip}$), and (d) the actions generated by our method. Compared to other methods, our method is optimal in generating hand action ("Drinking Water"), leg action ("Kicking Something"), and whole-body action ("Jump up"). In (a), (b), and (c), the "Drink Water" (first column) contains only the body morphology of the target action but not the hand moves of the source action. The "kicking Something" (second column) and "Jump up" (third column) combine the category features of the source action and the morphology features of the target action very well, but the hand moves are very raw. Our method generates more natural and coordinated actions, both in terms of the moves of the parts and the overall morphology.

To fully demonstrate that UMN is effective, we sampled 1% from $\mathcal{M}_{tr\hat{a}in}$ and generated actions using MGN and MGN+UMN, respectively. Then, it is tested according to the action recognition experiment (sec. 4.2). Table 4 shows that the average recognition accuracy is 81.48% for MGN+UMN and 64.96% for MGN. The results demonstrate that the UMN is effective.

5. Conclusion

In this paper, we propose a novel generative network called AGN by introducing active learning. AGN can generate many new actions by means of motion transfer with only one or a few samples. The AGN consists of the MGN and the UMN. The MGN is able to implicitly learn the skeletal morphology of the target action while preserving the category features of the source action. The UMN utilizes uncertainty-inspired learning in active learning to provide an uncertainty score for the generation process and thus guides the MGN to improve the quality of the generation. AGN showed the best performance compared to the existing methods. FMD is 2.67, and Accuracy is 92.18%.

References

[1] Kfir Aberman, Yijia Weng, Dani Lischinski, Daniel Cohen-Or, and Baoquan Chen. Unpaired motion style transfer from video to animation. *ACM Transactions on Graphics (TOG)*, 39(4):64–1, 2020. 1, 2, 5

[2] Jake K Aggarwal and Lu Xia. Human activity recognition from 3d data: A review. *Pattern Recognition Letters*, 48: 70–80, 2014. 1

[3] Antreas Antoniou, Amos Storkey, and Harrison Edwards. Data augmentation generative adversarial networks. *arXiv preprint arXiv:1711.04340*, 2017. 1

[4] Zhongyu Bai, Qichuan Ding, Hongli Xu, Jianning Chi, Xiangyue Zhang, and Tiansheng Sun. Skeleton-based similar action recognition through integrating the salient image feature into a center-connected graph convolutional network. *Neurocomputing*, 507:40–53, 2022. 1

[5] William H Beluch, Tim Genewein, Andreas Nürnberger, and Jan M Köhler. The power of ensembles for active learning in image classification. In *Proceedings of the IEEE conference on computer vision and pattern recognition*, pages 9368–9377, 2018. 3

[6] Jinmiao Cai, Nianjuan Jiang, Xiaoguang Han, Kui Jia, and Jiangbo Lu. Jolo-gcn: mining joint-centered light-weight information for skeleton-based action recognition. In *Proceedings of the IEEE/CVF winter conference on applications of computer vision*, pages 2735–2744, 2021. 1

[7] Joao Carreira and Andrew Zisserman. Quo vadis, action recognition? a new model and the kinetics dataset. In *proceedings of the IEEE Conference on Computer Vision and Pattern Recognition*, pages 6299–6308, 2017. 1

[8] Yunjey Choi, Minje Choi, Munyoung Kim, Jung-Woo Ha, Sunghun Kim, and Jaegul Choo. Stargan: Unified generative adversarial networks for multi-domain image-to-image translation. In *Proceedings of the IEEE conference on computer vision and pattern recognition*, pages 8789–8797, 2018. 1

[9] Yunjey Choi, Youngjung Uh, Jaejun Yoo, and Jung-Woo Ha. Stargan v2: Diverse image synthesis for multiple domains. In *Proceedings of the IEEE/CVF conference on computer vision and pattern recognition*, pages 8188–8197, 2020. 1

[10] Louis Clouâtre and Marc Demers. Figr: Few-shot image generation with reptile. *arXiv preprint arXiv:1901.02199*, 2019. 1

[11] Han Du, Erik Herrmann, Janis Sprenger, Klaus Fischer, and Philipp Slusallek. Stylistic locomotion modeling and synthesis using variational generative models. In *Proceedings of the 12th ACM SIGGRAPH Conference on Motion, Interaction and Games*, pages 1–10, 2019. 2

[12] Pan Du, Suyun Zhao, Hui Chen, Shuwen Chai, Hong Chen, and Cuiping Li. Contrastive coding for active learning under class distribution mismatch. In *Proceedings of the IEEE/CVF International Conference on Computer Vision*, pages 8927–8936, 2021. 2

[13] Sayna Ebrahimi, Mohamed Elhoseiny, Trevor Darrell, and Marcus Rohrbach. Uncertainty-guided continual learning with bayesian neural networks. *arXiv preprint arXiv:1906.02425*, 2019. 3

[14] Sergio Escalera, Vassilis Athitsos, and Isabelle Guyon. Challenges in multi-modal gesture recognition. *Gesture recognition*, pages 1–60, 2017. 1

[15] Christoph Feichtenhofer, Axel Pinz, and Andrew Zisserman. Convolutional two-stream network fusion for video action recognition. In *Proceedings of the IEEE conference on computer vision and pattern recognition*, pages 1933–1941, 2016. 1

[16] Christoph Feichtenhofer, Haoqi Fan, Jitendra Malik, and Kaiming He. Slowfast networks for video recognition. In *Proceedings of the IEEE/CVF international conference on computer vision*, pages 6202–6211, 2019. 1

[17] Chelsea Finn, Pieter Abbeel, and Sergey Levine. Model-agnostic meta-learning for fast adaptation of deep networks. In *International conference on machine learning*, pages 1126–1135. PMLR, 2017. 1

[18] Yarin Gal and Zoubin Ghahramani. Dropout as a bayesian approximation: Representing model uncertainty in deep learning. In *international conference on machine learning*, pages 1050–1059. PMLR, 2016. 3

[19] Yarin Gal, Riashat Islam, and Zoubin Ghahramani. Deep bayesian active learning with image data. In *International conference on machine learning*, pages 1183–1192. PMLR, 2017. 3

[20] Leon A Gatys, Alexander S Ecker, and Matthias Bethge. Image style transfer using convolutional neural networks. In *Proceedings of the IEEE conference on computer vision and pattern recognition*, pages 2414–2423, 2016. 2, 4

[21] Marc Gorriz, Axel Carlier, Emmanuel Faure, and Xavier Giró-i Nieto. Cost-effective active learning for melanoma segmentation. *arXiv preprint arXiv:1711.09168*, 2017. 3

[22] Fei Han, Brian Reily, William Hoff, and Hao Zhang. Space-time representation of people based on 3d skeletal data: A review. *Computer Vision and Image Understanding*, 158: 85–105, 2017. 1

[23] Zhezhi He, Adnan Siraj Rakin, and Deliang Fan. Parametric noise injection: Trainable randomness to improve deep neural network robustness against adversarial attack. In *Proceedings of the IEEE/CVF Conference on Computer Vision and Pattern Recognition*, pages 588–597, 2019. 1

[24] Jonathan Ho, Ajay Jain, and Pieter Abbeel. Denoising diffusion probabilistic models. *Advances in neural information processing systems*, 33:6840–6851, 2020. 1

[25] Daniel Holden, Jun Saito, and Taku Komura. A deep learning framework for character motion synthesis and editing. *Acm Transactions on Graphics*, 35(4):1–11, 2016. 1, 2, 5

[26] Yan Hong, Li Niu, Jianfu Zhang, and Liqing Zhang. Matchinggan: Matching-based few-shot image generation. In *2020 IEEE International conference on multimedia and expo (ICME)*, pages 1–6. IEEE, 2020. 1

[27] Yan Hong, Li Niu, Jianfu Zhang, Weijie Zhao, Chen Fu, and Liqing Zhang. F2gan: Fusing-and-filling gan for few-shot image generation. In *Proceedings of the 28th ACM international conference on multimedia*, pages 2535–2543, 2020.

[28] Yan Hong, Li Niu, Jianfu Zhang, and Liqing Zhang. Deltagan: Towards diverse few-shot image generation with sample-specific delta. In *European Conference on Computer Vision*, pages 259–276. Springer, 2022. 1

[29] Xun Huang and Serge Belongie. Arbitrary style transfer in real-time with adaptive instance normalization. In *Proceedings of the IEEE international conference on computer vision*, pages 1501–1510, 2017. 1

[30] Deok-Kyeong Jang, Soomin Park, and Sung-Hee Lee. Motion puzzle: Arbitrary motion style transfer by body part. *ACM Transactions on Graphics (TOG)*, 41(3):1–16, 2022. 1, 2, 3, 4, 5

[31] Shuiwang Ji, Wei Xu, Ming Yang, and Kai Yu. 3d convolutional neural networks for human action recognition. *IEEE transactions on pattern analysis and machine intelligence*, 35(1):221–231, 2012. 1

[32] Tero Karras, Samuli Laine, and Timo Aila. A style-based generator architecture for generative adversarial networks. In *Proceedings of the IEEE/CVF conference on computer vision and pattern recognition*, pages 4401–4410, 2019. 1, 2

[33] Tero Karras, Samuli Laine, Miika Aittala, Janne Hellsten, Jaakko Lehtinen, and Timo Aila. Analyzing and improving the image quality of stylegan. In *Proceedings of the IEEE/CVF conference on computer vision and pattern recognition*, pages 8110–8119, 2020. 1, 2

[34] Durk P Kingma and Prafulla Dhariwal. Glow: Generative flow with invertible 1x1 convolutions. *Advances in neural information processing systems*, 31, 2018. 1

[35] Diederik P Kingma and Max Welling. Auto-encoding variational bayes. *arXiv preprint arXiv:1312.6114*, 2013. 1

[36] Maosen Li, Siheng Chen, Xu Chen, Ya Zhang, Yanfeng Wang, and Qi Tian. Actional-structural graph convolutional networks for skeleton-based action recognition. In *Proceedings of the IEEE/CVF conference on computer vision and pattern recognition*, pages 3595–3603, 2019. 1

[37] Huidong Liu, Xianfeng Gu, and Dimitris Samaras. Wasserstein gan with quadratic transport cost. In *Proceedings of the IEEE/CVF international conference on computer vision*, pages 4832–4841, 2019. 1

[38] Nan Liu, Shuang Li, Yilun Du, Antonio Torralba, and Joshua B Tenenbaum. Compositional visual generation with composable diffusion models. In *European Conference on Computer Vision*, pages 423–439. Springer, 2022. 1

[39] Romain Lopez, Jeffrey Regier, Michael I Jordan, and Nir Yosef. Information constraints on auto-encoding variational bayes. *Advances in neural information processing systems*, 31, 2018. 1

[40] Romain Lopez, Pierre Boyeau, Nir Yosef, Michael Jordan, and Jeffrey Regier. Decision-making with auto-encoding variational bayes. *Advances in Neural Information Processing Systems*, 33:5081–5092, 2020. 1

[41] Dwarikanath Mahapatra, Behzad Bozorgtabar, Jean-Philippe Thiran, and Mauricio Reyes. Efficient active learning for image classification and segmentation using a sample selection and conditional generative adversarial network. In *International Conference on Medical Image Computing and Computer-Assisted Intervention*, pages 580–588. Springer, 2018. 3

[42] Xudong Mao, Qing Li, Haoran Xie, Raymond YK Lau, Zhen Wang, and Stephen Paul Smolley. Least squares generative adversarial networks. In *Proceedings of the IEEE inter-national conference on computer vision*, pages 2794–2802, 2017. 1

[43] Christoph Mayer and Radu Timofte. Adversarial sampling for active learning. In *Proceedings of the IEEE/CVF Winter Conference on Applications of Computer Vision*, pages 3071–3079, 2020. 3

[44] Olof Mogren. C-rnn-gan: Continuous recurrent neural networks with adversarial training. *arXiv preprint arXiv:1611.09904*, 2016. 2

[45] Hieu T Nguyen and Arnold Smeulders. Active learning using pre-clustering. In *Proceedings of the twenty-first international conference on Machine learning*, page 79, 2004. 3

[46] Alex Nichol and John Schulman. Reptile: a scalable metalearning algorithm. *arXiv preprint arXiv:1803.02999*, 2(3): 4, 2018. 1

[47] Xingang Pan, Ayush Tewari, Thomas Leimkühler, Lingjie Liu, Abhimitra Meka, and Christian Theobalt. Drag your gan: Interactive point-based manipulation on the generative image manifold. In *ACM SIGGRAPH 2023 Conference Proceedings*, pages 1–11, 2023. 2

[48] ParkSoomin, JangDeok-Kyeong, and LeeSung-Hee. Diverse motion stylization for multiple style domains via spatial-temporal graph-based generative model. *Proceedings of the ACM on Computer Graphics and Interactive Techniques*, 2021. 1, 2, 3, 5

[49] Or Patashnik, Zongze Wu, Eli Shechtman, Daniel Cohen-Or, and Dani Lischinski. Styleclip: Text-driven manipulation of stylegan imagery. In *Proceedings of the IEEE/CVF International Conference on Computer Vision*, pages 2085–2094, 2021. 2

[50] Alec Radford, Luke Metz, and Soumith Chintala. Unsupervised representation learning with deep convolutional generative adversarial networks. *arXiv preprint arXiv:1511.06434*, 2015. 1, 2

[51] Danilo Rezende and Shakir Mohamed. Variational inference with normalizing flows. In *International conference on machine learning*, pages 1530–1538. PMLR, 2015. 1

[52] Kuniaki Saito, Kate Saenko, and Ming-Yu Liu. Coco-funit: Few-shot unsupervised image translation with a content conditioned style encoder. In *Computer Vision–ECCV 2020: 16th European Conference, Glasgow, UK, August 23–28, 2020, Proceedings, Part III 16*, pages 382–398. Springer, 2020. 1, 2, 4

[53] Masaki Saito, Eiichi Matsumoto, and Shunta Saito. Temporal generative adversarial nets with singular value clipping. In *Proceedings of the IEEE international conference on computer vision*, pages 2830–2839, 2017. 2

[54] Amir Shahroudy, Jun Liu, Tian-Tsong Ng, and Gang Wang. Ntu rgb+ d: A large scale dataset for 3d human activity analysis. In *Proceedings of the IEEE conference on computer vision and pattern recognition*, pages 1010–1019, 2016. 3

[55] Xuning Shao and Weidong Zhang. Spatchgan: A statistical feature based discriminator for unsupervised image-to-image translation. In *Proceedings of the IEEE/CVF International Conference on Computer Vision*, pages 6546–6555, 2021. 2

[56] Lei Shi, Yifan Zhang, Jian Cheng, and Hanqing Lu. Two-stream adaptive graph convolutional networks for skeleton-based action recognition. In *Proceedings of the IEEE/CVF*

conference on computer vision and pattern recognition, pages 12026–12035, 2019. 1

[57] Connor Shorten and Taghi M Khoshgoftaar. A survey on image data augmentation for deep learning. *Journal of big data*, 6(1):1–48, 2019. 1

[58] Karen Simonyan and Andrew Zisserman. Very deep convolutional networks for large-scale image recognition. *arXiv preprint arXiv:1409.1556*, 2014. 3

[59] Samarth Sinha, Sayna Ebrahimi, and Trevor Darrell. Variational adversarial active learning. In *Proceedings of the IEEE/CVF International Conference on Computer Vision*, pages 5972–5981, 2019. 2

[60] Yael Vinker, Eliahu Horwitz, Nir Zabari, and Yedid Hoshen. Image shape manipulation from a single augmented training sample. In *Proceedings of the IEEE/CVF International Conference on Computer Vision*, pages 13769–13778, 2021. 2

[61] Carl Vondrick, Hamed Pirsiavash, and Antonio Torralba. Generating videos with scene dynamics. *Advances in neural information processing systems*, 29, 2016. 2

[62] Jiayu Wang, Wengang Zhou, Jinhui Tang, Zhongqian Fu, Qi Tian, and Houqiang Li. Unregularized auto-encoder with generative adversarial networks for image generation. In *Proceedings of the 26th ACM international conference on Multimedia*, pages 709–717, 2018. 1

[63] Pichao Wang, Wanqing Li, Philip Ogunbona, Jun Wan, and Sergio Escalera. Rgb-d-based human motion recognition with deep learning: A survey. *Computer vision and image understanding*, 171:118–139, 2018. 1

[64] Shihong Xia, Congyi Wang, Jinxiang Chai, and Jessica Hodgins. Realtime style transfer for unlabeled heterogeneous human motion. *ACM Transactions on Graphics (TOG)*, 34 (4):1–10, 2015. 2

[65] Sijie Yan, Yuanjun Xiong, and Dahua Lin. Spatial temporal graph convolutional networks for skeleton-based action recognition. In *Proceedings of the AAAI conference on artificial intelligence*, 2018. 1

[66] Sijie Yan, Zhizhong Li, Yuanjun Xiong, Huahan Yan, and Dahua Lin. Convolutional sequence generation for skeleton-based action synthesis. In *Proceedings of the IEEE/CVF International Conference on Computer Vision*, pages 4394–4402, 2019. 3

[67] Hao Yang, Chunfeng Yuan, Bing Li, Yang Du, Junliang Xing, Weiming Hu, and Stephen J Maybank. Asymmetric 3d convolutional neural networks for action recognition. *Pattern recognition*, 85:1–12, 2019. 1

[68] Lin Yang, Yizhe Zhang, Jianxu Chen, Siyuan Zhang, and Danny Z Chen. Suggestive annotation: A deep active learning framework for biomedical image segmentation. In *Medical Image Computing and Computer Assisted Intervention-MICCAI 2017: 20th International Conference, Quebec City, QC, Canada, September 11-13, 2017, Proceedings, Part III 20*, pages 399–407. Springer, 2017. 3

[69] M Ersin Yumer and Niloy J Mitra. Spectral style transfer for human motion between independent actions. *ACM Transactions on Graphics (TOG)*, 35(4):1–8, 2016. 2

[70] Beichen Zhang, Liang Li, Shijie Yang, Shuhui Wang, Zheng-Jun Zha, and Qingming Huang. State-relabeling adversarial active learning. In *Proceedings of the IEEE/CVF conference on computer vision and pattern recognition*, pages 8756–8765, 2020. 2

[71] Yuxin Zhang, Nisha Huang, Fan Tang, Haibin Huang, Chongyang Ma, Weiming Dong, and Changsheng Xu. Inversion-based style transfer with diffusion models. In *Proceedings of the IEEE/CVF Conference on Computer Vision and Pattern Recognition*, pages 10146–10156, 2023. 1

[72] Jia-Jie Zhu and José Bento. Generative adversarial active learning. *arXiv preprint arXiv:1702.07956*, 2017. 3